Supplementary Information for

Altering the structures of 3D supramolecular assemblies from melamine and cyanuric acid derivatives in water

Nikita Orekhov, Nina Bukhtiiarova, Zlata A. Brushevich, Anton A. Muravev, Nadav Elad, Yael Tsarfati, Anna Kossoy, Isai Feldman, Anastasia Zelenina, Anna A. Rubekina, Sergey N. Semenov* and Ekaterina V. Skorb*

*Correspondence to: sergey.semenov@weizmann.ac.il; skorb@itmo.ru

Table of Contents

Materials and Methods

Cyanuric chloride, melamine, ammonia solution (25%), methylamine hydrochloride, cyanuric acid, mesyl chloride, 5-hexyl-1-ol, triethylamine, 1,8-Diazabicyclo(5.4.0)undec-7-ene (DBU), and sodium sulfate were purchased from Sigma-Aldrich, Acros Organics, Alfa Aesar, and Merck. Solvents – dichloromethane (DCM), methanol, acetone, and anhydrous DMF were purchased from Sigma-Aldrich and Acros Organics. D_2O was purchased form Tzamal d-chem; all other NMR solvents were purchased from Cambridge Isotope Laboratories. All chemicals, including solvents, were used without further purification.

NMR spectra were measured on a Bruker AVANCE III-300 spectrometer at 300 MHz for ^1H and on a Bruker AVANCE III-400 spectrometer at 400 MHz for ^1H. Chemical shifts for ^1H are given in ppm relative to TMS. ^1H and spectra were calibrated using a residual solvent peak as an internal reference. Data for the ^1H NMR spectra were reported as follows: chemical shift (ppm), peak shape (s = singlet, d = doublet, t = triplet, q = quartet, p = pentet, m = multiplet, br = broad, dd = doublet of doublets), coupling constant (Hz), and integration.

The Chromatographic separation and mass analysis were performed on a Waters Acquity liquid chromatography system equipped with a PDA Detector (210 and 700 nm) and a Waters QDa mass detector with an electrospray ionization (ESI) and a mass range of 85–1250 m/z

Synthesis

6-chloro-1,3,5-triazine-2,4-diamine

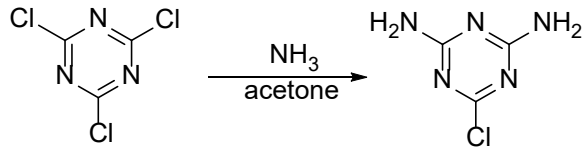

Under stirring, a hot suspension of cyanuric trichloride (20g, 54 mmol) in acetone (100 mL) was added to 65 mL of 25 wt% ammonia (130 mmol) in 100g of crushed ice

while the temperature was below 10 °C. After complete addition, the temperature was raised to 40-50 °C and reaction mixture was stirred for 4 hours. Then, the reaction mixture was cooled to room temperature and filtered. The white solid was washed with H_2O and dried in *vacuo* at 40°C. The product was identified by HPLC MS.

N^2-methyl-1,3,5-triazine-2,4,6-triamine (N-methylmelamine, **MM**)

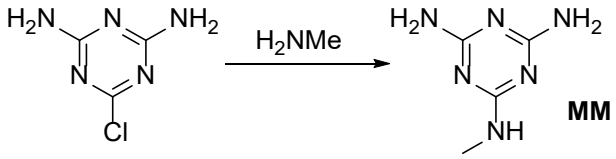

6-chloro-1,3,5-triazine-2,4-diamine (1.0 g, 6.85 mmol) was suspended in 10 ml of water, then methylamine hydrochloride (0.92 g, 13,7 mmol) and NaOH (0.82 g, 20.55 mmol) in water (10 ml) were added. The mixture was stirred at reflux for 2 h. After the mixture had cooled to room temperature, the solid was filtered off, washed with water, and dried under *vacuo* at 40°C.

1H NMR (300 MHz, DMSO) δ, ppm: 6.4 (q, 1H), 6.2 (s, 2H), 6.0 (s, 2H), 2.7 (d, 3H). Spectrum matched the literature values.[1]

1-(hex-5-yn-1-yl)-1,3,5-triazinane-2,4,6-trione (hexynyl-cyanuric acid, **HCA**)

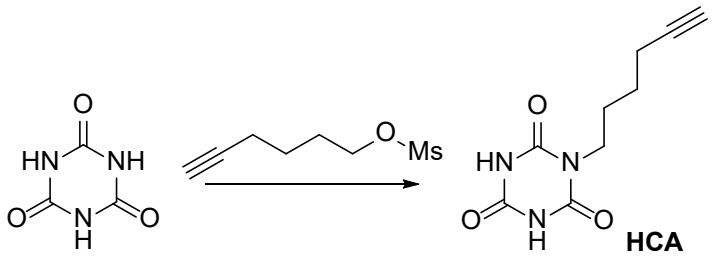

HCA was prepared according to the modified literature protocol.[2] First, Hex-5-yn-1-yl methanesulfonate was prepared according to the following procedure. Mesyl chloride (1.8 ml, 23 mmol) was added dropwise to a stirring solution of 5-hexyl-1-ol (1.69 ml, 15.3 mmol) and Et_3N (3.2 ml, 23 mmol) in anhydrous DCM (40 ml) at 0°C under Argon atmosphere. After 3 hours, water (40 mL) was added. The organic layer was washed with water, dried over Na_2SO_4 and concentrated to give Hex-5-yn-1-yl methanesulfonate as a yellow oil.

1H NMR (300 MHz, DMSO) δ, ppm: 4.2 (t, 2H), 3.2 (s, 3H), 2.8 (p, 1H), 2.2 (td 2H), 1.8 (p, 2H), 1.5 (p, 2H).

Cyanuric acid (1.3 g, 10 mmol) and hex-5-yn-1-yl methanesulfonate (350 mg, 2 mmol) were dissolved in anhydrous DMF (25 ml), and DBU (300 µl, 2 mmol) was added dropwise. Then reaction mixture was stirred at 130ºC for 36 hours. An inert atmosphere was maintained during the reaction. After completion of the reaction, DMF was removed in *vacuo,* and the residue was dissolved in MeOH and filtered to remove an excess of cyanuric acid. Resulting solution was concentrated and purified by a filtration through a silica plug using 20:1 DCM/MeOH as eluent, to give **HCA** as a pale yellow solid.

1H NMR (400 MHz, DMSO) δ, ppm: 3.64 (t, 2H), 2.74 (t, 1H), 2.17 (td 2H), 1.60 (p, 2H), 1.42 (p, 2H). Spectrum matched the literature values.[2]

Powder X-ray diffraction measurements

X-ray diffraction (XRD) measurements were performed at ambient using Rigaku (Tokyo, Japan) θ-θ diffractometers: an Ultima III, equipped with a capillary head and with a sealed Cu anode tube operating at 40 kV/40 mA, and a TTRAX III, equipped with an Eulerian cradle (Multipurpose Attachment, Rigaku – MPA) and a rotating Cu anode X-ray tube operating at 50 kV/200 mA. Both diffractometers were equipped with a scintillation detector that was aligned to intersect the diffracted beam after it had passed the graphite monochromator to sufficiently reduce K_β radiation.

For a 1 mm diameter capillary, it was used a nearly parallel focused X-ray beam (0.05° divergence angle), formed by a multilayered mirror (Rigaku, Cross Beam Optics attachment) and confined to a 1 mm incident slit. The Eulerian cradle allowed us to scan in reflection and transmission geometries using a primary X-ray beam formed by a 0.25 degree incident and scattering slits and a 0.6 mm receiving slit. 2theta/theta specular scanning was performed in the 2θ range from 1° to 60° with step size of 0.025° and a scan rate of 1° per minute.

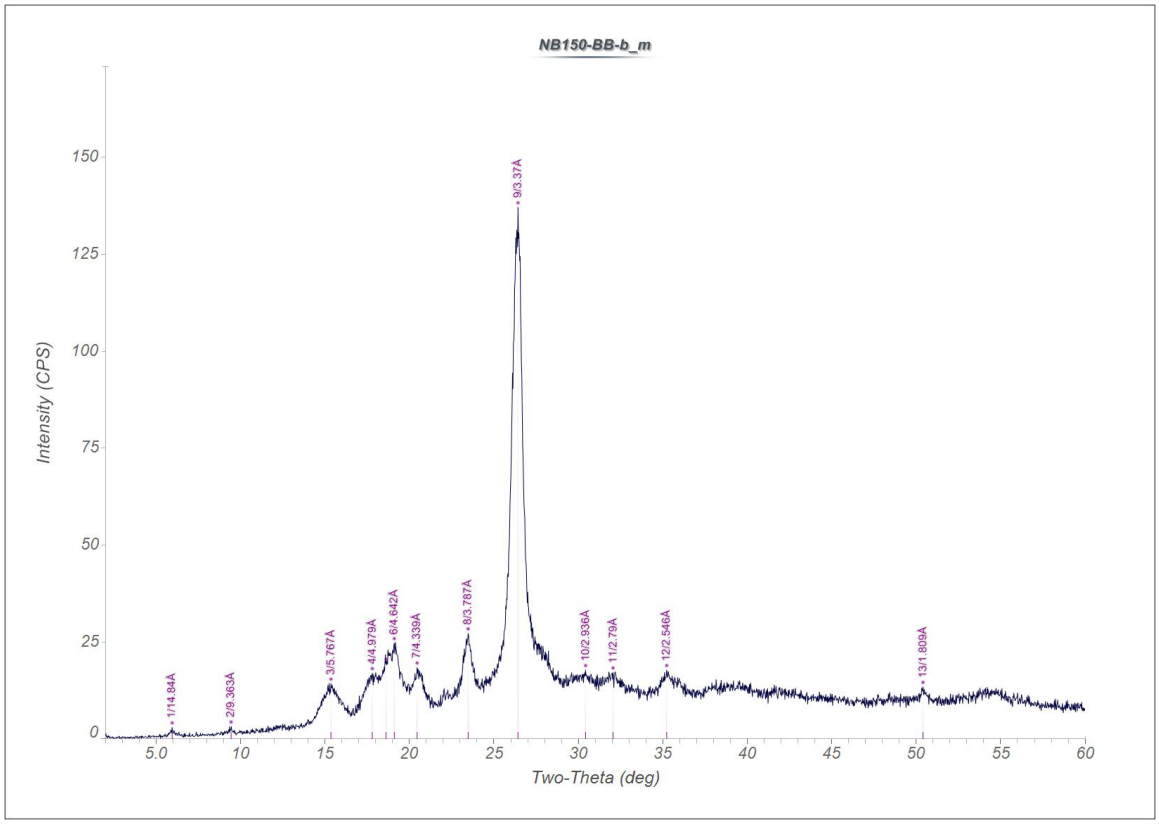

Figure S1. XRD pattern for **MM·HCA** sample obtained by fast mixing of water solutions of MM (10 mM) and HCA (10 mM) at room temperature.

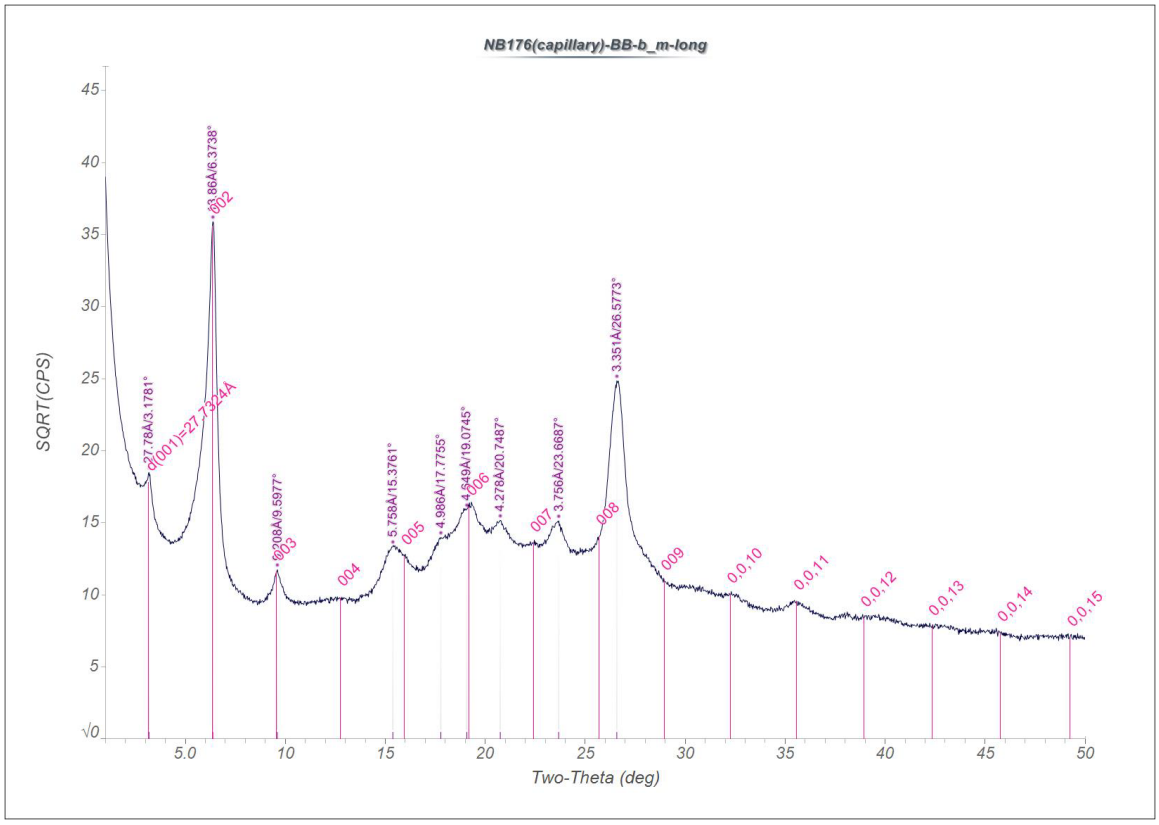

Figure S2. XRD pattern for **MM·HCA** sample in capillary. This sample was obtained by the same procedure as the sample used to obtain XRD pattern in Figure 2 of the main text.

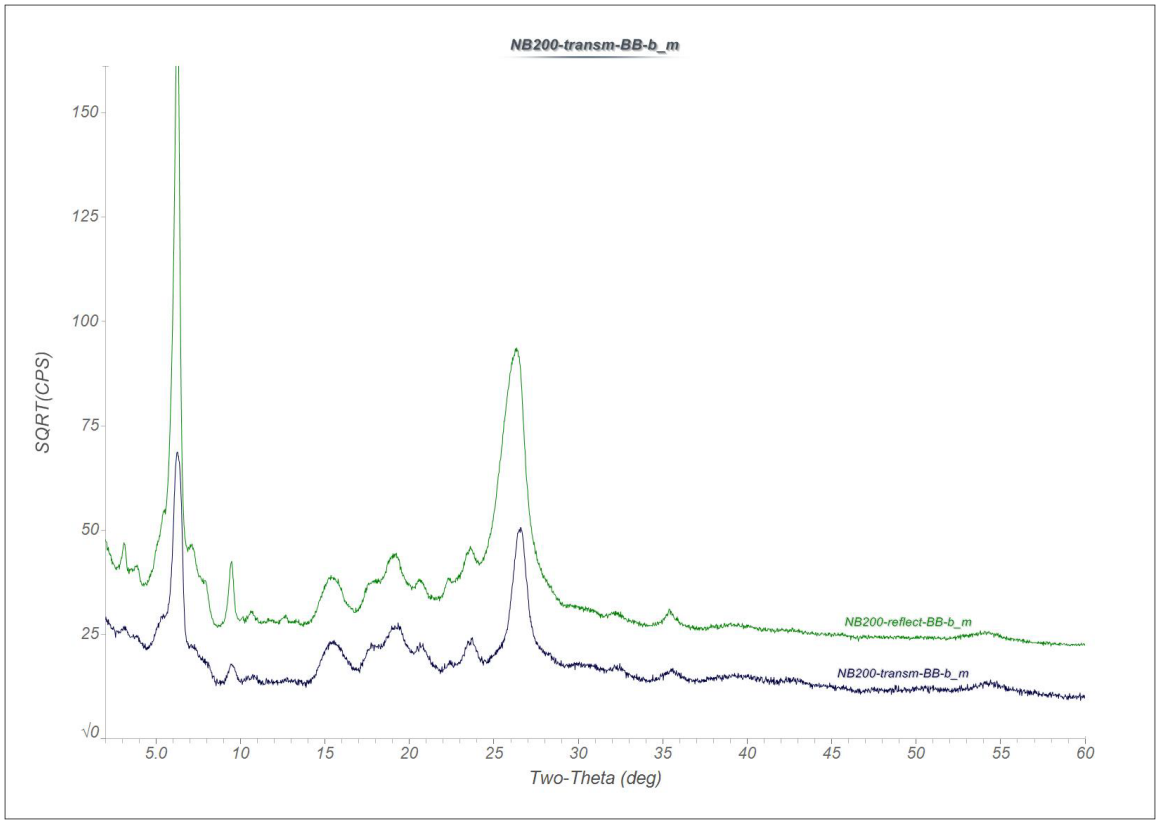

Figure S3. The comparison of XRD patterns for a **MM·HCA** sample obtained in reflection (green) and transmission (blue) modes. This sample was obtained by the same procedure as the sample used to obtain XRD pattern in Figure 2 of the main text.

Scanning electron microscopy (SEM) measurements

Particles images were acquired on ESEM (environmental electron microscope) Quattro S by Thermo Fisher Scientific in SE (secondary electron) mode with Everhart-Thornley detector in high vacuum. Accelerating voltage was 2 kV.

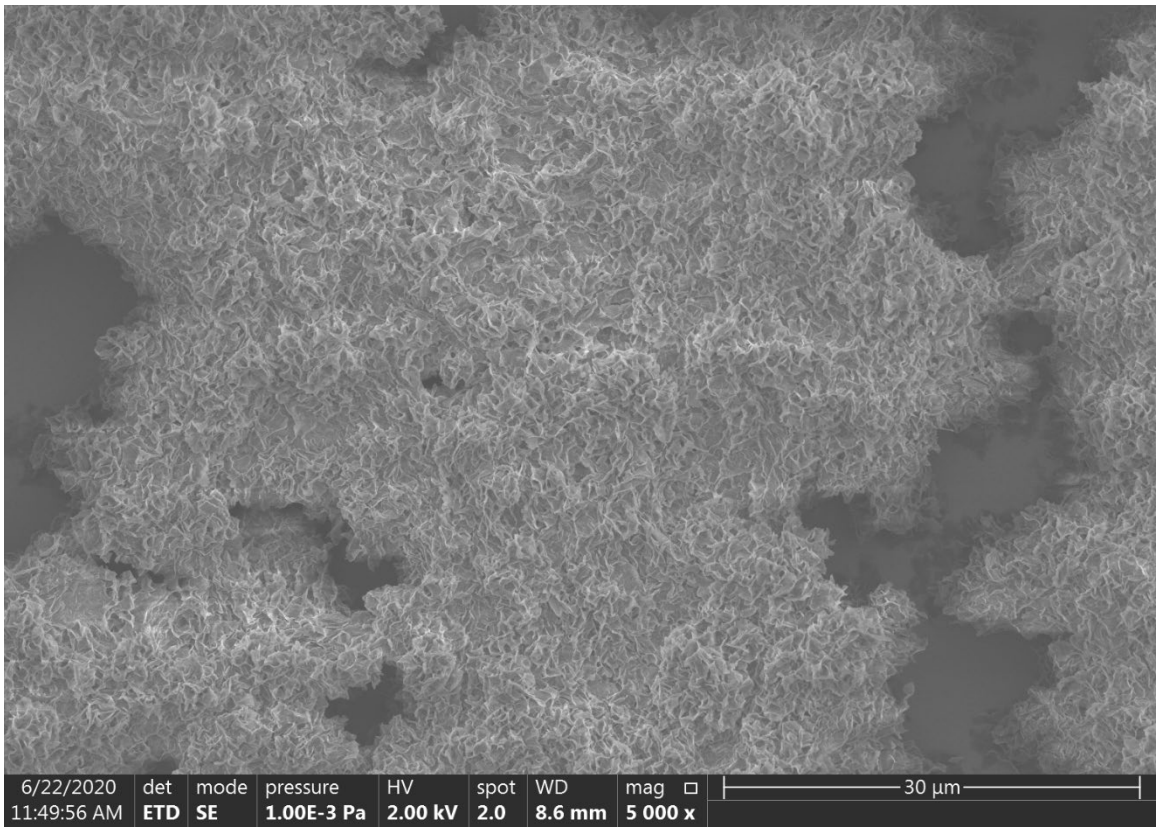

Figure S4. SEM image of **M·HCA** sample obtained by slow cooling of the mixture of M (10 mM) and HCA (10 mM) water solutions.

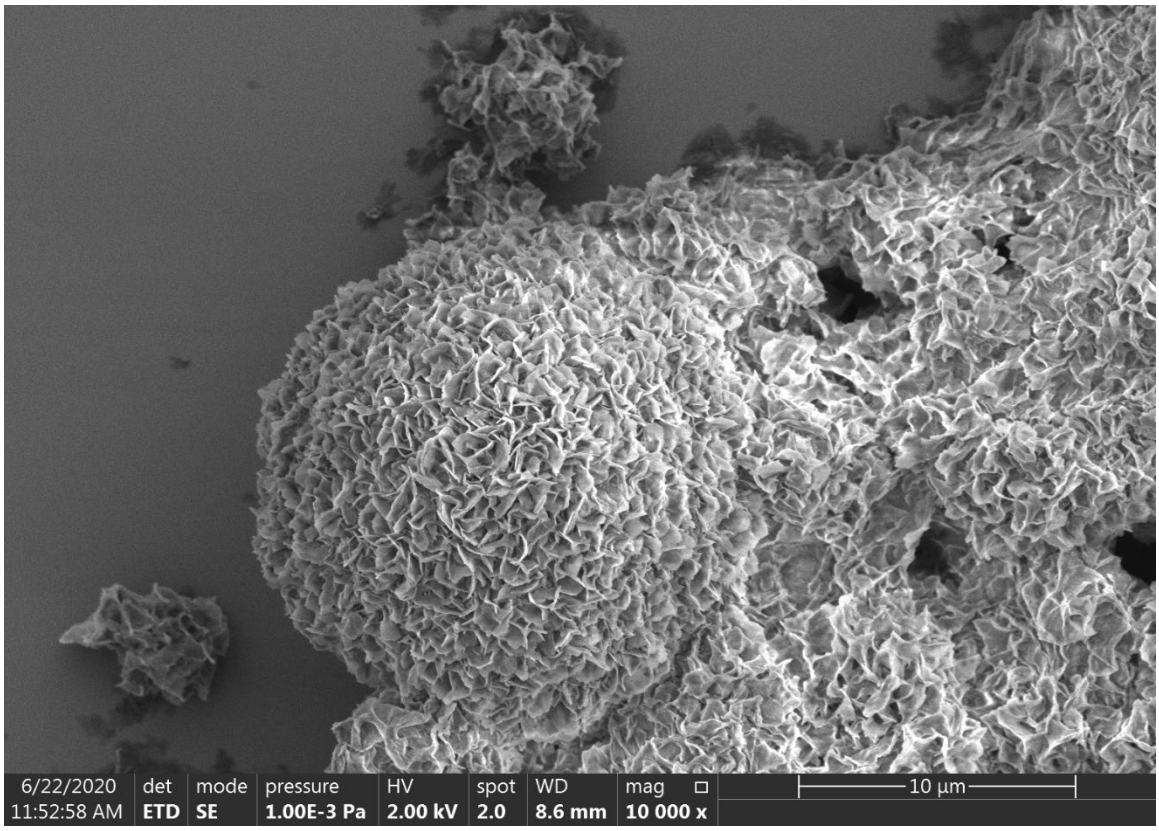

Figure S5. Another SEM image of **M·HCA** sample obtained by slow cooling of the mixture of M (10 mM) and HCA (10 mM) water solutions.

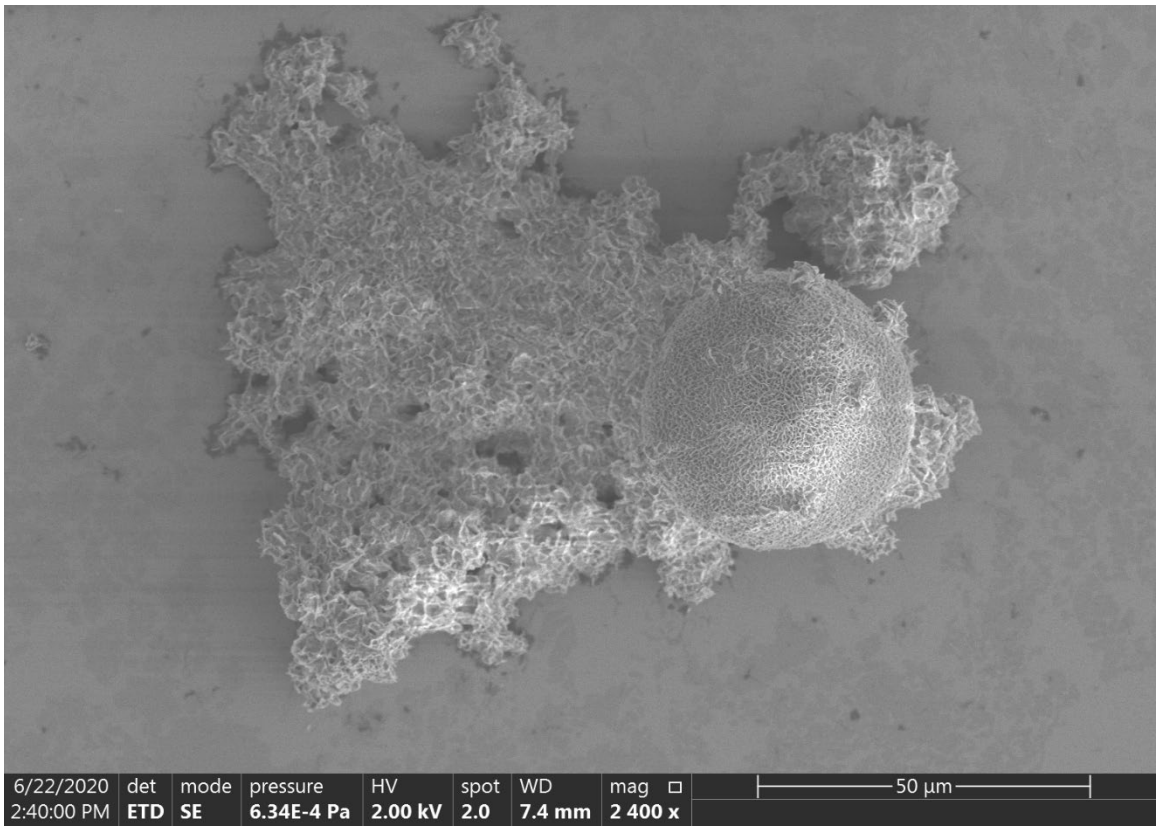

Figure S6. SEM image of **MM·HCA** sample obtained by slow cooling of the mixture of MM (10 mM) and HCA (10 mM) water solutions.

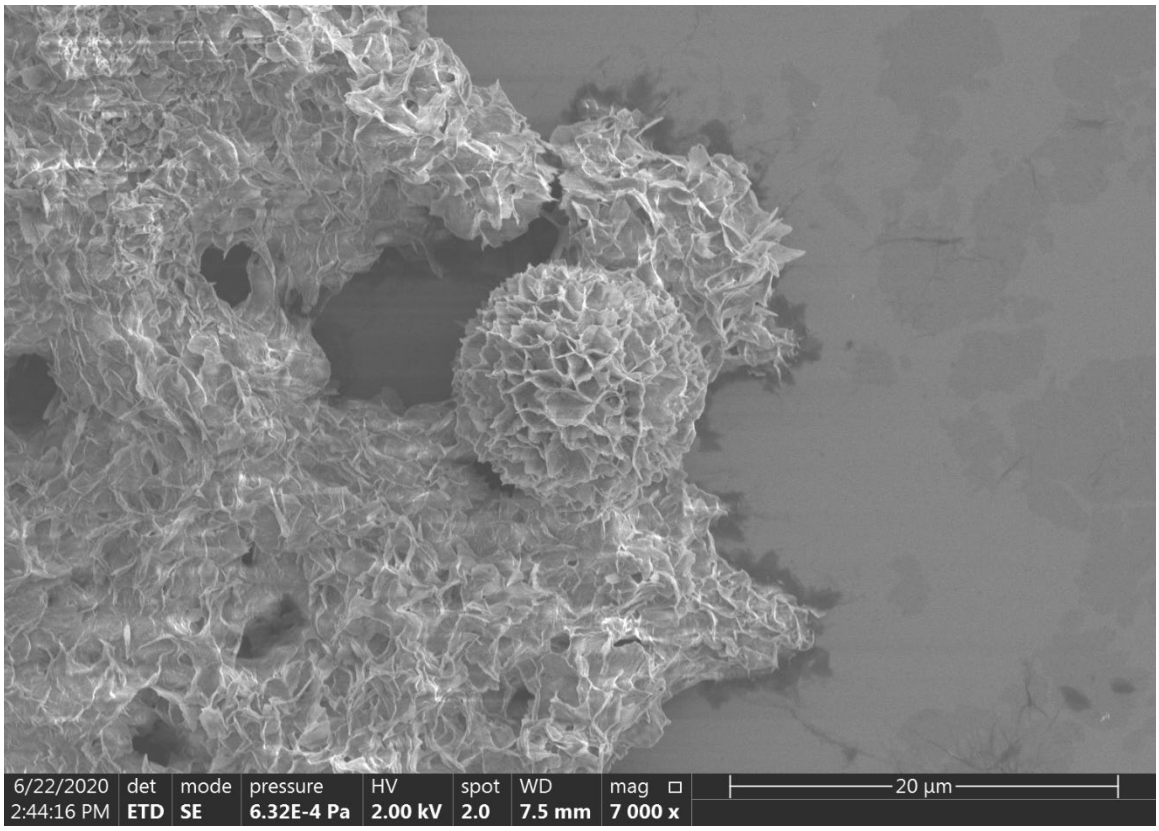

Figure S7. SEM image of **MM·HCA** sample obtained by slow cooling of the mixture of MM (10 mM) and HCA (10 mM) water solutions.

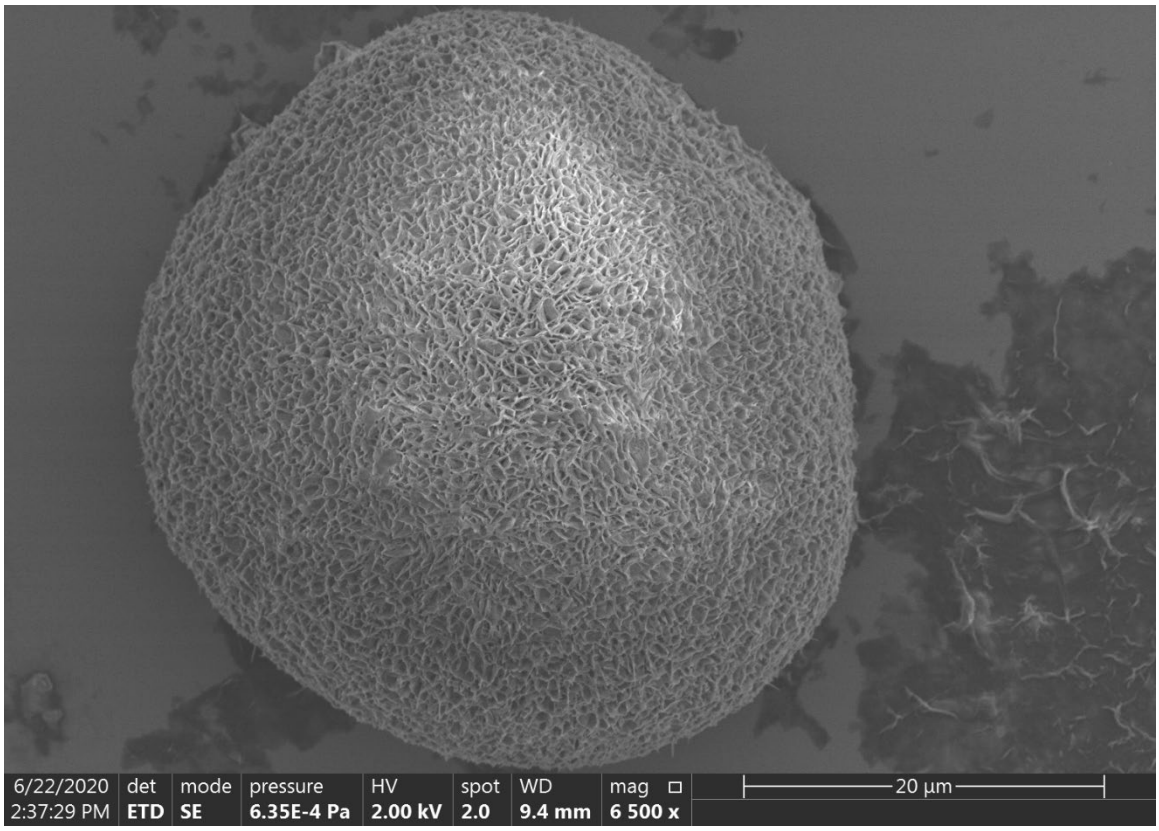

Figure S8. SEM image of **MM·HCA** sample obtained by slow cooling of the mixture of MM (10 mM) and HCA (10 mM) water solutions.

Transmission electron microscopy (TEM) measurements

TEM specimens of **M·HCA** and **MM·HCA** were prepared in two ways. First way involved applying 3.5 μL of sample (obtained by mixing M or MM solution (5 mM) with HCA solution (5 mM)) onto glow-discharged holey carbon grids (Pacific Grid-Tech), blotted for 2.6 seconds at 93% humidity, and plunge frozen in liquid ethane cooled by liquid nitrogen using an EM-GP plunger (Leica). Second way involved applying 3.5 μL of sample (obtained as described above) onto glow-discharged holey carbon grids (Pacific Grid-Tech) and drying it at ambient conditions. Grids were loaded onto a Titan Krios TEM (Thermo Fisher Scientific) and imaged under liquid nitrogen temperature at an acceleration voltage of 300 kV. Imaging was done on a K3 direct detector mounted behind a BioQuantum energy filter (Gatan). For **MM·HCA** the best images were obtained using the first protocol.For **M·HCA** the best images were obtained using the second protocol.

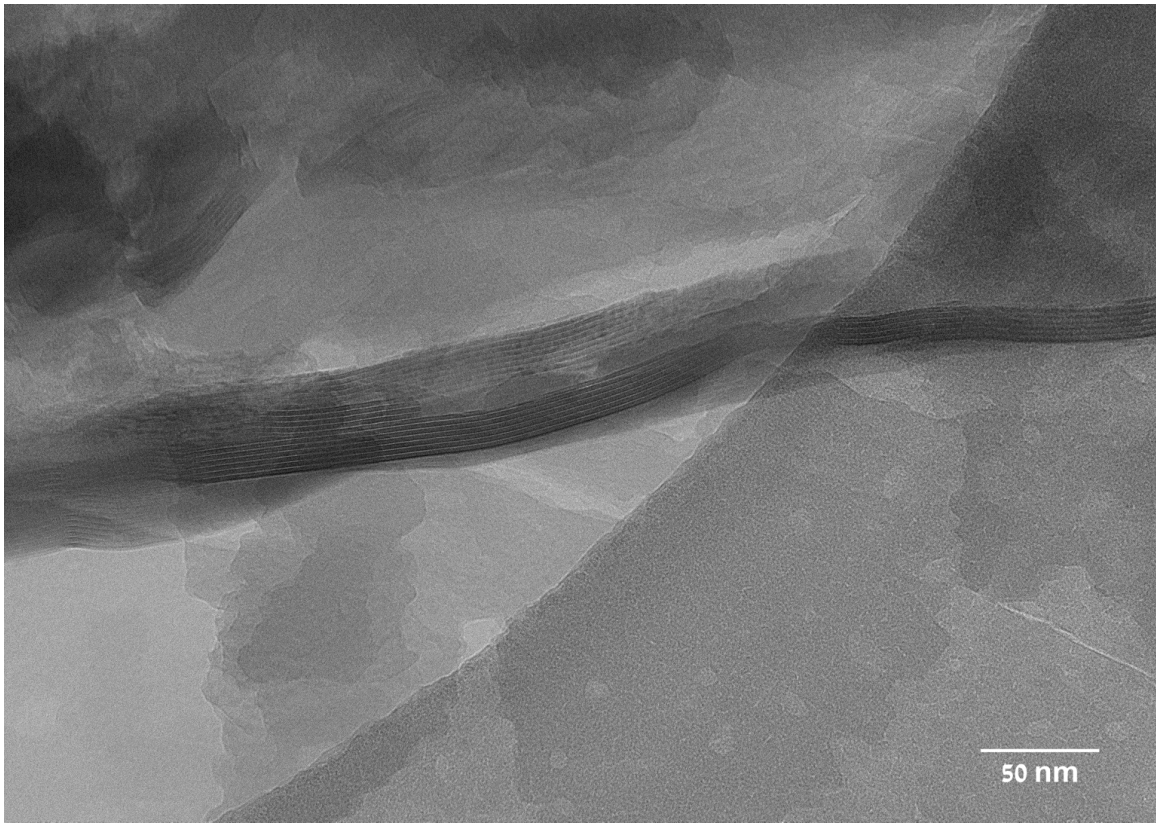

Figure S9. TEM image of **M·HCA** sample obtained in the second way. It is the full view of the image analyzed in Figure 3a.

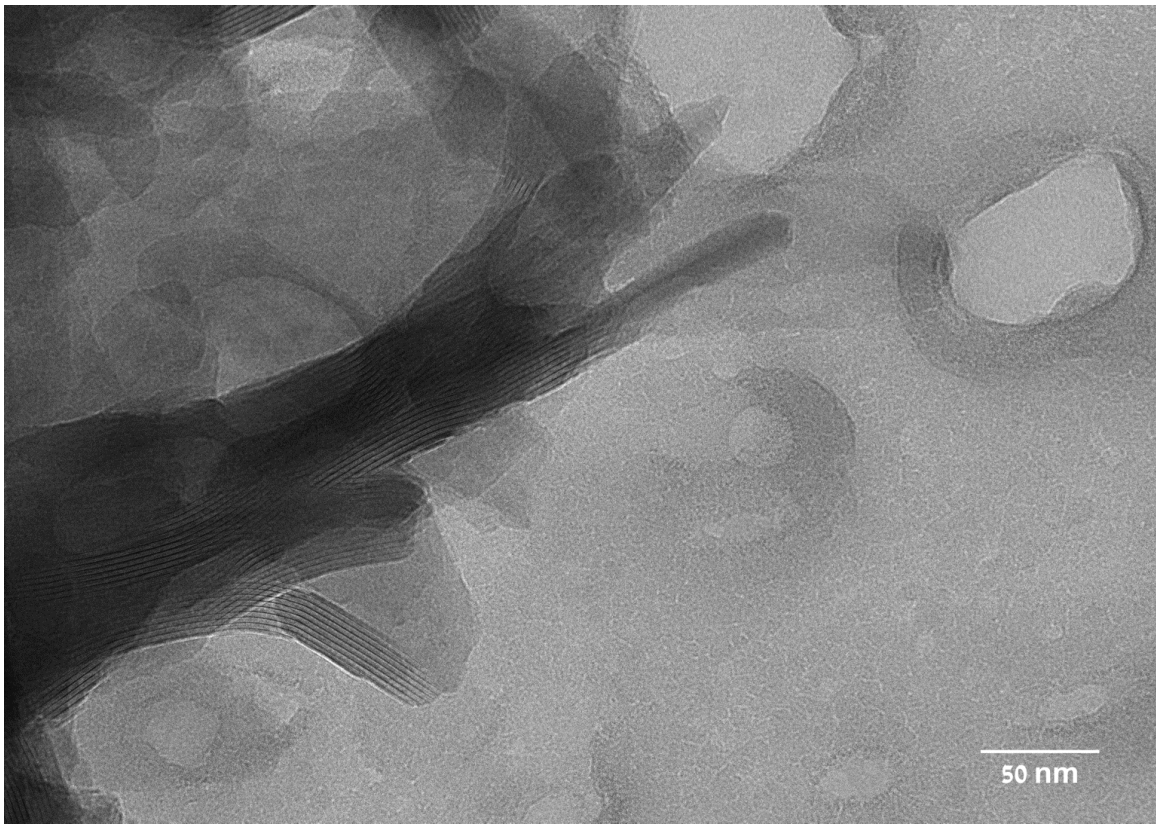

Figure S10. TEM image of the same **M·HCA** sample as in Figure S9, but taken in different location.

Molecular dynamics (MD) simulations

We performed MD simulations of M and CA assembly using GROMACS package.[3]To describe interatomic interactions, we applied the OPLS-AA force field[4]with partial charges parameterized by LigParGen.[5] The TIP4P[6] rigid nonpolarizable model was used to parameterize the water molecules. A cutoff for short-range and nonbonded interactions was 1.2 nm. For long-range Coulomb interactions, we used the smooth Particle-Mesh Ewald scheme.[7]Visualization was produced using VMD.[8]

To analyze the growth mechanisms for both types of molecular arrangements we performed 500ns-long constant-temperature/constant-pressure simulations at T = 300 K and P = 1 atm for M*HCA and MM*HCA. The computational cell with periodic boundary conditions containing initial crystal surrounded by water (Fig. S11a,b) and every 50 ns ten pairs of molecules (M + HCA or MM + HCA) were inserted into solution. Eventually these molecules were absorbed on the surface of the initial crystal starting the growth process.

To characterize the level of crystallinity of the newly-formed layers we compute Hermans' structure factor for every new molecule in that layer:

$$P = \frac{1}{n}\sum_{i=1}^{n}\frac{3\cos^2\Theta_i - 1}{2}$$

where Θ_i is an angle between the vector orthogonal to aromatic ring of i-th molecule and (1,0,0) vector. Ordered structures are characterized by higher values of *P*, while random orientation gives *P*=0. Fig. S11c shows the evolution of the structure factor for both systems. For M*HCA crystal, which is characterized by larger energy difference between head-to-tail and tail-to-tail arrangements, we observe proper orientation of molecules in newly formed layers, while for MM*HCA these layers are more amorphous. The latter can be attributed to the smaller timescale in comparison with real experiment, which does not give enough time for molecules to arrange properly.

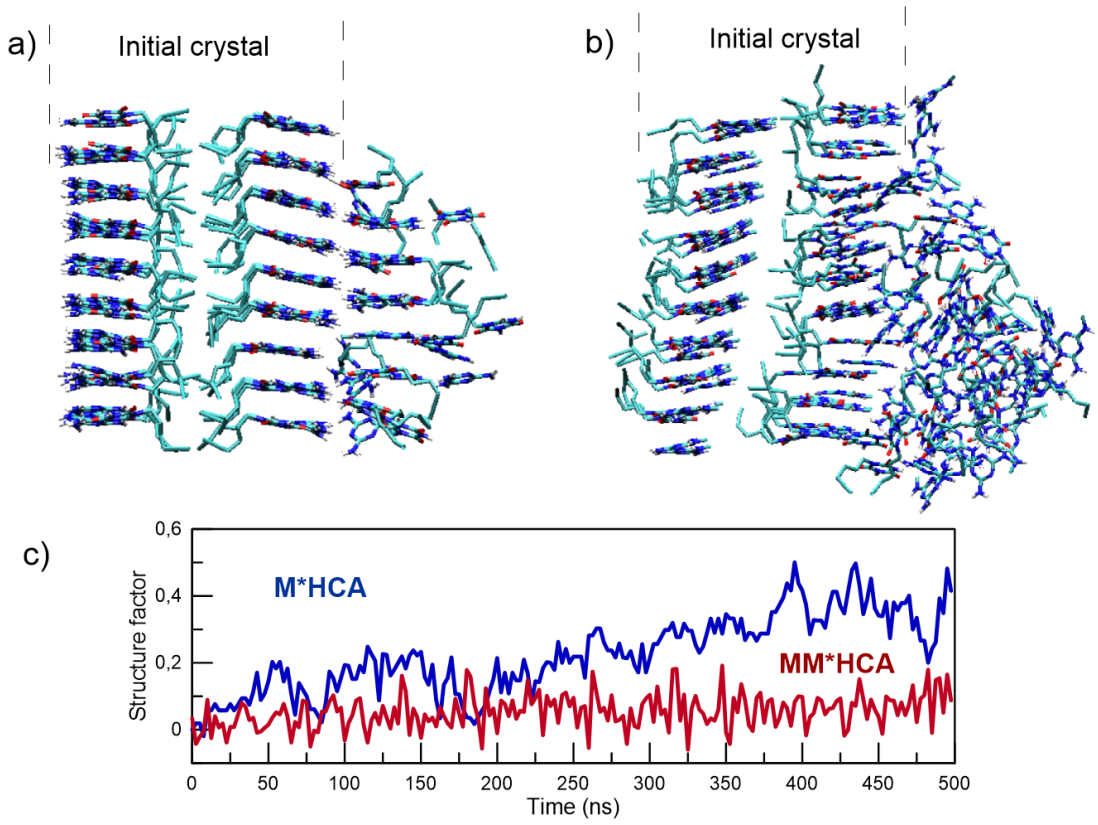

Figure S11. Final atomistic structure of crystal surface for a) **M·HCA** and b) **MM·HCA** after 500 ns MD simulation. c) Evolution of structure factor during the growth of both types of crystals.

References

1. M. List, H. Puchinger, H. Gabriel, U. Monkowius and C. Schwarzinger, *J. Org. Chem.*, 2016, **81**, 4066-4075.
2. Y. Wang, P. J. Santos, J. M. Kubiak, X. Guo, M. S. Lee and R. J. Macfarlane, *J. Am. Chem. Soc.*, 2019, **141**, 13234-13243.
3. E. Lindahl, B. Hess, D. van der Spoel, GROMACS 3.0: a package for molecular simulation and trajectory analysis. *Mol. Modell. Annu.***7**, 306–317 (2001).
4. W. L. Jorgensen, D. S. Maxwell, J. Tirado-Rives, Development and testing of the OPLS all-atom force field on conformational energetics and properties of organic liquids. *J. Am. Chem. Soc.***118**, 11225–11236 (1996).
5. L. S. Dodda, I. C. de Vaca, J. Tirado-Rives, W. L. Jorgensen, LigParGen web server: an automatic OPLS-AA parameter generator for organic ligands. *Nucl. Acid Res.***45**, W331–W336 (2017).
6. W. L. Jorgensen, J. Chandrasekhar, J. D. Madura, R. W. Impey, M. L. Klein, Comparison of simple potential functions for simulating liquid water. *J. Chem. Phys.***79**, 926–935 (1983).
7. U. Essmann, L. Perera, M. L. Berkowitz, T. Darden, H. Lee, L. G. Pedersen, A smooth particle mesh Ewald method. *J. Chem. Phys.***103**, 8577–8593 (1995).
8. W. Humphrey, A. Dalke, K. Schulten, VMD: Visual molecular dynamics. *J. Mol. Graph.***14**, 33–38 (1996).